

## Flow-velocity Microsensors Based on Semiconductor Field-effect Structures

Arshak Poghossian<sup>1</sup>, Tatsuo Yoshinobu<sup>2</sup> and Michael J. Schöning<sup>1,3\*</sup>

<sup>1</sup>Institute of Thin Films and Interfaces, Research Centre Jülich, D-52425 Jülich, Germany

<sup>2</sup>Institute of Scientific and Industrial Research, Osaka University, 8-1 Mihogaoka, Ibaraki, Osaka 567-0047, Japan

<sup>3</sup>University of Applied Sciences, Aachen, Division Jülich, Ginsterweg 1, D-52428, Jülich, Germany

\* Author to whom correspondence should be addressed ([M.J.Schoening@fz-juelich.de](mailto:M.J.Schoening@fz-juelich.de)).

Received: 18 May 2003 / Accepted: 24 June 2003 / Published: 27 July 2003

---

**Abstract:** A time-of-flight-type flow-velocity sensor employing the in-situ electrochemically generation of ion-tracers is developed. The sensor consists of an ion generator and two downstream-placed pH-sensitive Ta<sub>2</sub>O<sub>5</sub>-gate ISFETs (ion-sensitive field-effect transistor) that detect generated H<sup>+</sup>- or OH<sup>-</sup>-ions. The results of the developed flow-velocity sensor under different modes of ion generation are presented and discussed. By applying this ISFET-array, the time of flight, and consequently, the flow velocity can be accurately evaluated using the shift of the response curve of the respective ISFETs in the array along the time scale. A good linearity between the measured flow velocity with the ISFET-array and the delivered flow rate of the pump is observed. In addition, a possibility of flow-velocity measurements by means of a LAPS (light-addressable potentiometric sensor) is firstly demonstrated.

**Keywords:** Flow-velocity sensor, time of flight, ISFET, LAPS, pH, ion generation.

---

### Introduction

Over the last decade many efforts have been expended to create miniaturised liquid flow sensors using semiconductor and micromachining technologies. Potential fields of applications of these sensors

include flow injection analysis, integrated fluid analysis systems such as  $\mu$ TAS (micro total analysis system), lab-on-chip and electronic tongue devices for industrial process control, biomedical instrumentation, drug delivery system, etc.. It is obvious that for a successful commercial realisation, the micro flow sensors should have a simple design and functional principle, high reliability, small dimensions, high accuracy, fast response time and wide working range.

Different transducer principles have been proposed and realised for micro flow sensors. A review of recent advances in micromachined liquid flow sensors can be found in [1,2]. The most widely used functional principles are differential pressure detection [3,4], thermal dilution in a flow stream [5-7] and time of flight (or thermal transit time) measurement of a heat impulse injected into the flow [5,8]. The time-of flight type thermal flow sensor is accurate and stable due to its sensing mechanism. However, because it requires a relatively high heat pulse, additional technological processes are needed for a good thermal isolation of the heater. Therefore, an ion drug method [9], in-situ electrochemically producing of bubbles [10] as well as oxygen [11] have been also suggested for flow-rate or flow-velocity detection in liquids.

As an alternative to flow sensors which apply the bubbles or oxygen-producing methods, recently, a new concept for a "time-of-flight"-type flow-velocity and flow-direction sensor that is based on in-situ electrochemical generation of ion tracers and an ISFET (ion-sensitive field-effect transistor) as ion-tracer detector, has been introduced and realised by the authors [12-14]. Such an ISFET-based flow sensor has a simple operation principle and uses a dynamic measuring method (i.e., only relative changes in the sensor's output signal are of interest and thus, the detector's drift, temperature instability and sensitivity discrepancy between the various ISFETs are not relevant). Moreover, due to the fast response time of the ISFET (usually in the millisecond range), it can be utilised for flow-velocity measurements in a wide range from  $\mu\text{m/s}$  up to  $\text{m/s}$ .

However, when using a single ISFET as an ion-concentration detector, there are some difficulties to accurately determine the time of flight, i.e. the time difference between the ion generation and the detection of the generated ions by the ISFET, which will mainly define the accuracy of the flow-velocity measurements. Therefore, in this work, we propose a flow-velocity sensor based on an ISFET array, where the time of flight and thus, the flow velocity can be determined with sufficient high precision using the shift of position of the response curves of different ISFETs in the array. In addition, a possibility of flow-velocity measurements by means of a LAPS (light-addressable potentiometric sensor) and capacitive EIS (electrolyte-insulator.semiconductor) sensor is discussed.

## Functional principle

The functional principle of the time-of-flight-type flow-velocity sensor based on an ISFET array is schematically shown in Fig. 1. The sensor consists of a chemical tracer generator (e.g., Pt- or Au-electrode for the  $\text{H}^+$ - or  $\text{OH}^-$ -ion generation due to electrolysis of water) and a downstream-placed ion-detector, here, an array of ISFETs (for simplicity, an array consisting of two ISFETs is considered), that detects the in-situ electrochemically generated chemical tracers. At the time  $t_g$ , an electrical pulse is applied to the ion generator and the respective ions are produced at the generator electrode. After being produced, the  $\text{H}^+$ - or  $\text{OH}^-$ -ions will be transported to the downstream-placed ISFET array by

convection and are detected there. Since the ISFET output signal (detector signal) will be defined by the pH value in the gate region, the shape and amount of change of the ISFET output signal will be determined by the mode of ion-generation, the number of generated ions as well as by diffusion effects in the case of an extremely low flow velocity. In particular, in the case of the ion-pulse generation, the peaks will be formed in a way, as it is schematically shown in Fig. 1(b).

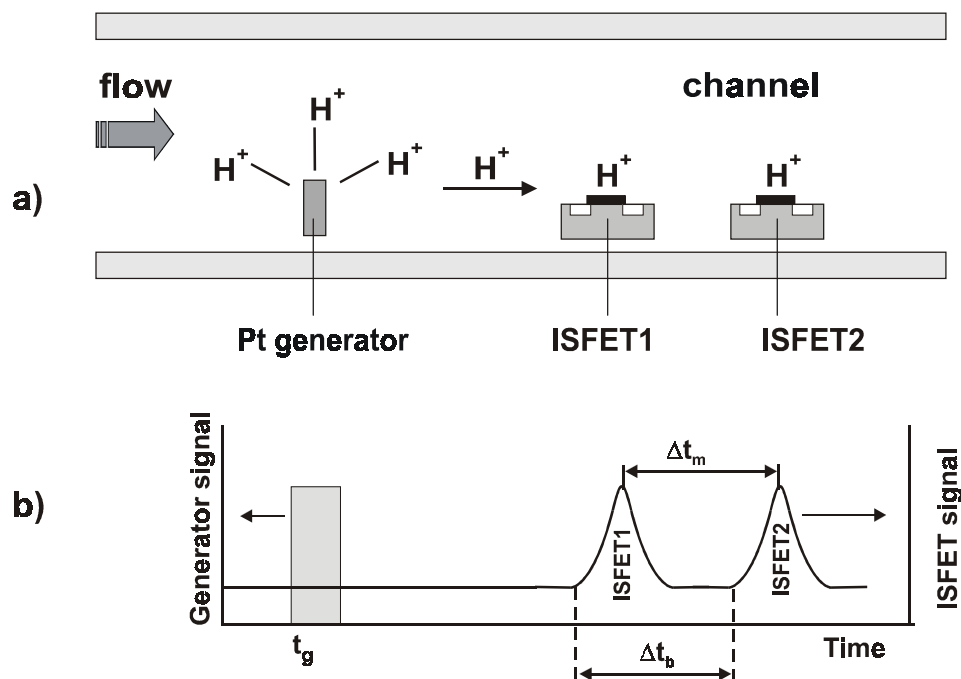


**Figure 1.** Flow-velocity sensor based on an ISFET array (schematically): a) functional principle, b) time of flight measurement.

In an ideal case, i.e. when the ISFETs have identical intrinsic characteristics, and the deformation of the ion pulse during transportation due to diffusion and convection processes can be neglected, the response curves of different ISFETs in the array will have the same shape but will be shifted along the time scale. This shift, i.e. the time of flight, will be inversely proportional to the flow velocity. Thus, by a given distance between the ISFETs, the flow velocity can be accurately evaluated using, for example, the time difference between the time moments of beginning of the signal change of the two ISFETs ( $\Delta t_b$ ) or the time difference of signal maxima ( $\Delta t_m$ ) of the two ISFETs (see Fig. 1(b)).

## Experimental

Flow-velocity measurements have been performed using the measuring system, which has been developed in our group for the multi-parameter detection of different (bio-)chemical/physical quantities utilising the ISFET as a basic transducer [15]. It combines an ISFET module, a flow-through cell, a pump, an ISFET-meter, a voltage source (for ion generation) and is completely driven by a personal computer. Fig. 2 shows the developed ISFET module before encapsulation. It combines two pH-

sensitive ISFETs and an upstream-placed ion generator (Au film or Pt wire (not shown)), which are integrated onto a printed circuit board. The pH ISFETs used are n-channel (meander-shaped with ~3 mm in width and 30  $\mu\text{m}$  in length) devices with  $\text{Ta}_2\text{O}_5$ -gate as a pH-sensitive material. The gate composite insulator consists of a ~80 nm  $\text{SiO}_2$  layer, covered by a ~80 nm thick  $\text{Ta}_2\text{O}_5$  film. The ISFET chip size was 2 mm x 3.2 mm. The whole module except the sensitive regions, is encapsulated using epoxy compound. The resulting sensitive area of the ISFETs was about 0.5-1  $\text{mm}^2$  and the distance between the middle of two ISFET's gates was ~9 mm.

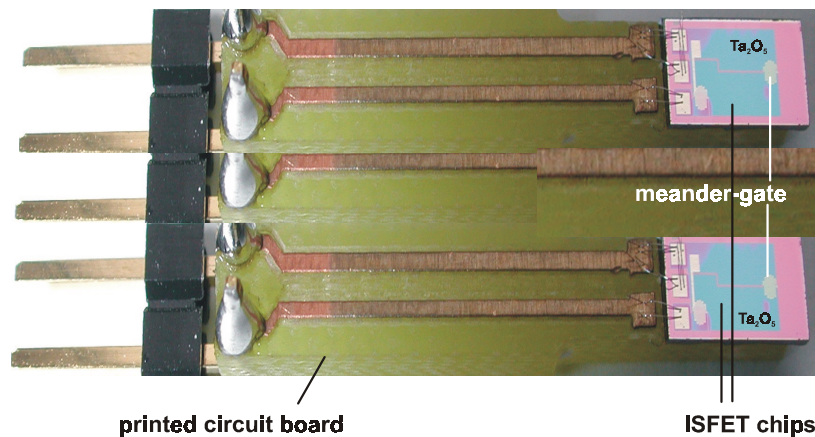


**Figure 2.** Photo of the ISFET module before encapsulation.

For the sensor characterisation, the ISFET module has been horizontally positioned on the bottom of a rectangular channel of the flow-through cell with channel size of 2 mm in width and 0.5 mm in height. A common Ag/AgCl miniature reference electrode and a counter electrode have been placed in the same flow-through cell. The counter electrode (Pt wire) was positioned downstream of the ISFETs and at a distance large enough to prevent an influence of the produced counter ions. The test solution (unbuffered 0.1 M  $\text{KNO}_3$  water solution, pH 7) is pumped through the channel by the pump “MS-1 Reglo 160” (Ismatec, Wertheim-Mondfeld, Germany) providing a flow rate in the range from 0.005 to 45 ml/min. Before flow-velocity measurements, the pH ISFETs have been characterised under both static and flow-through conditions using standard pH buffer solutions. A typical response is linear between pH 2 and pH 12 with a slope of 55-58 mV/pH. For some experimental details, see [12-14].

The ISFET array-based flow-velocity sensor has been tested for both  $\text{H}^+$ - and  $\text{OH}^-$ -ion generation. Two different modes of ion generation have been applied: a long-time generation up to reach a relatively constant sensor output signal, and a short ion-pulse generation (15 s) by a constant generation current of 30  $\mu\text{A}$ . Flow-velocity measurements have been carried out by means of the constant charge method with a grounded reference electrode using a home-made ISFET-meter (Research Centre Jülich). Measurements were performed at room temperature.

### Sensor response under long-time ion generation

Fig. 3(a) demonstrates the typical output signal of the two ISFETs, downstream-placed of the generator, versus the time at different flow rates from 0.1 to 0.6 ml/min. In this experiment,  $\text{OH}^-$ -ions

were generated up to reach a constant sensor signal. The arrows in Fig. 3(a) mark the time of the beginning (arrows downwards) and the end of generation (arrows upwards). After the ion generation, it takes some delay time  $t_i$  before the induced OH<sup>-</sup>-ions reach the gate region of the respective ISFET by convection and will be, then, detected there. As a result, the sensor signal after the time period  $t_i$  is first decreased and then, saturated because the ion-generation process is still continued. A similar effect has been observed after switching off the ion generator. It takes some delay time before the induced pH change passes the gate region of the respective ISFET. As a result, the sensor signal is increased and recovers to its initial value. The ISFET output signal changes were about 180-200 mV. Considering a pH sensitivity for the ISFET of 56 mV/pH, this voltage shift corresponds to a pH change near the ISFET gate region of about  $\Delta\text{pH}\sim 3.2\text{-}3.5$ . Due to a certain voltage drop across the test solution between the generator and the counter electrode, some electrical artefact has been observed (the stepwise change in the sensor signal at the time moments of the beginning and the end of the ion generation), which, however, does not influence the results of the flow-velocity measurements.

As expected, both ISFETs show identical response curves, which, however, are shifted along the time scale because of the different distance between the generator electrode and the respective ISFET. As it can be clearly seen from Fig. 3(b), with increasing the flow rate, the time  $\Delta t_b = t_2 - t_1$  that is needed for the generated ions to “fly” from the gate region of ISFET1 to the gate region of ISFET2, is decreased. Thus, the flow velocity can be determined using the respective values of  $\Delta t_b$ , evaluated for different flow rates.

In this experiment, the time of flight,  $\Delta t_b$ , was evaluated as the time difference between the time moments of beginning of the signal change of the two ISFETs. The time moment of beginning of the signal change was taken from the intersection points of the interpolated middle value of the respective ISFET's signal after the ion generation and the tangent at the inflection point of the response curve (this procedure is shown in Fig. 3(b)). The corresponding calibration curve of the sensor, evaluated for different flow rates from 0.1 to 0.6 ml/min, will be discussed later (see also Fig. 5).

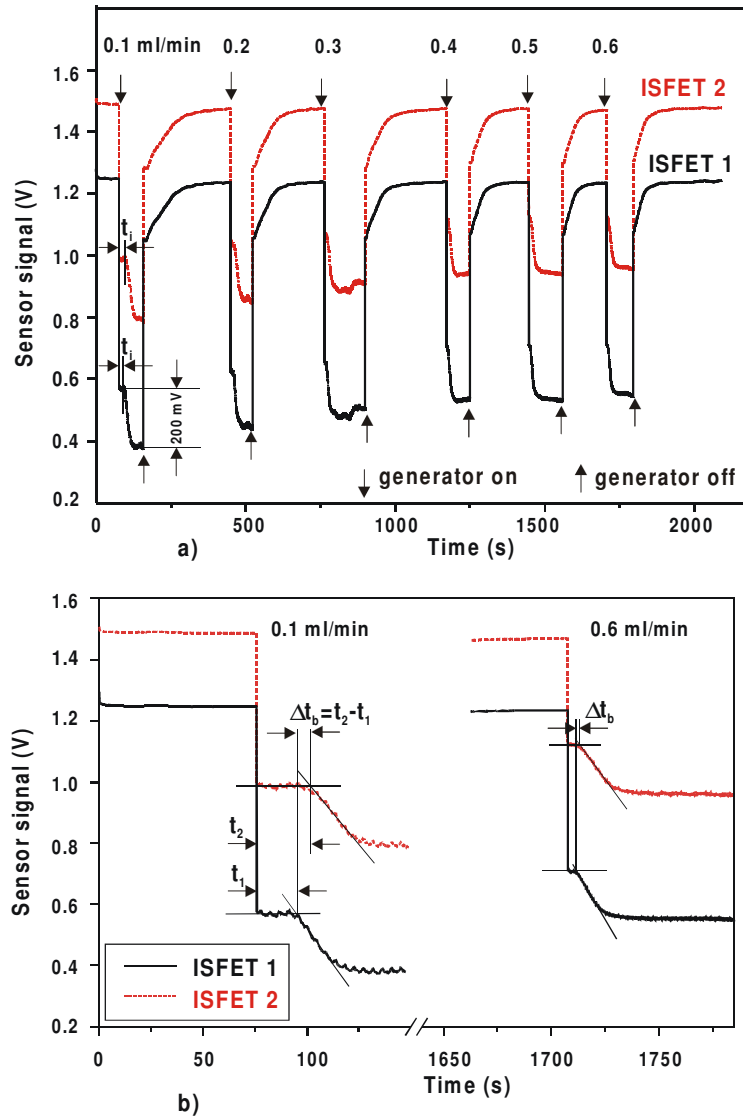
### Sensor response under short ion-pulse generation

Fig. 4(a) shows the typical response of the two ISFETs under short ion-pulse generation at different flow rates from 0.1 to 0.5 ml/min. In this experiment, the H<sup>+</sup>-ion pulse has been generated at a constant current of 30  $\mu\text{A}$  for about 15 s.

The arrows in Fig. 4(a) mark the time of beginning of ion generation. Also here, after the ion-pulse generation, it takes some delay time before the induced pH change reaches the downstream-placed ISFETs. The ISFETs' output signal changes were about 50-60 mV, which corresponds to a pH change near the ISFETs gate region of about  $\Delta\text{pH}\sim 1$ . These values of signal change and corresponding pH change are less than in the case of the long-time ion generation, which can be explained by the smaller amount of generated ions due to the short duration of ion generation.

As expected, when passing the ion pulse over the respective ISFET, peaks in the sensor output signal are observed, and after that, each output signal recovers to its initial value. The widths of the signal peaks are dependent on the flow rate. The smaller the flow rate, the wider the signal peak. Moreover, the widths of the peaks are much larger than the duration of the ion pulse ( $\sim 15$  s), because

the ion pulse is deformed and broadened during the transportation as well as due to the relatively large sensitive gate area ( $\sim 0.5\text{-}1\text{ mm}^2$ ) of the ISFETs. Although the amplitudes of the signal peaks differ slightly due to the deformation of the ion pulse as well as due to possible small discrepancies in the pH sensitivity of the ISFETs, the positions of these maxima depend on the flow velocity (flow rate) only. With increasing the flow rate, the time difference between the signal maxima of the two ISFETs ( $\Delta t_m$ ) decreases. As it can be clearly seen from Fig. 4(b), at a flow rate of 0.1 ml/min, the  $\Delta t_m$  value is much larger than for a flow rate of 0.5 ml/min. Therefore, in this experiment, the time of flight has been



**Figure 3.** Typical output signal of the flow-velocity sensor consisting of two ISFETs at different flow rates from 0.1 to 0.6 ml/min (a) and determination of the time of flight (b). In this experiment,  $\text{OH}^-$  ions were generated by a constant current of  $30\ \mu\text{A}$  up to reach a constant sensor signal. The arrows mark the time of the beginning (arrows downwards) and the end of ion generation (arrows upwards).  $t_b$ : time of flight that is needed for the generated  $\text{OH}^-$  ions to “fly” from ISFET1 to ISFET2;  $t_i$ : time difference between the time moments of ion generation and beginning of the signal change of the ISFET.

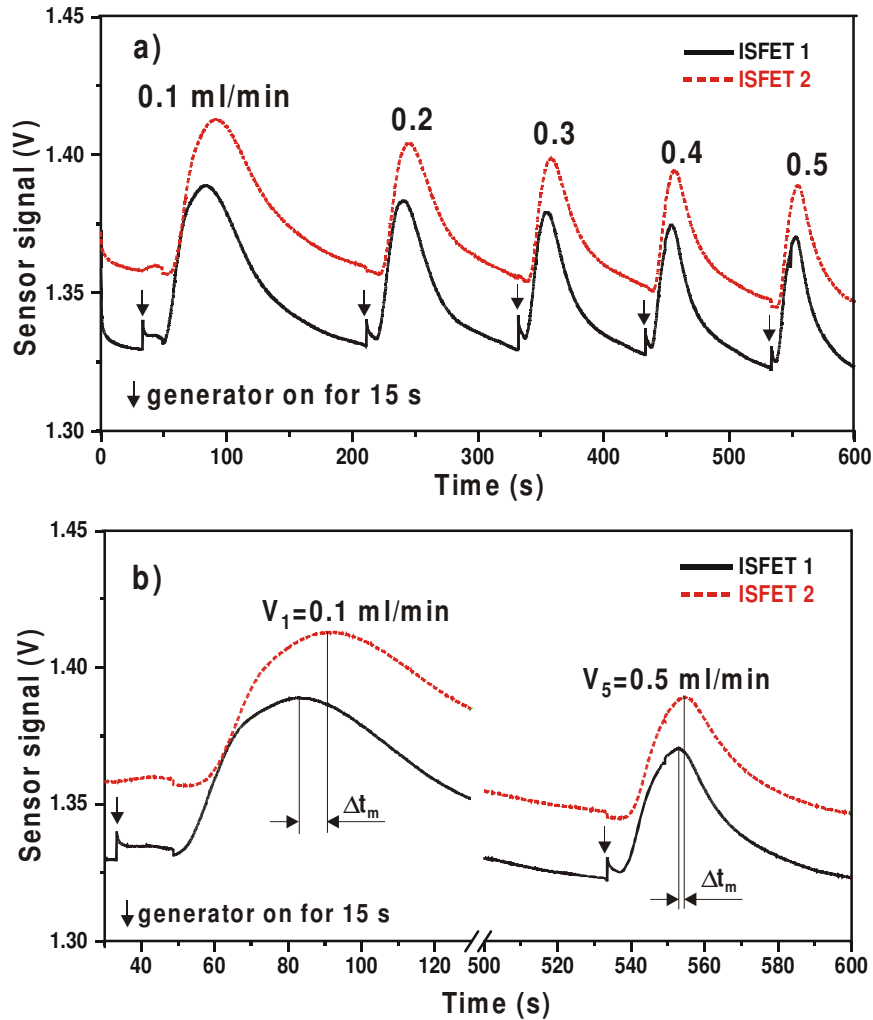


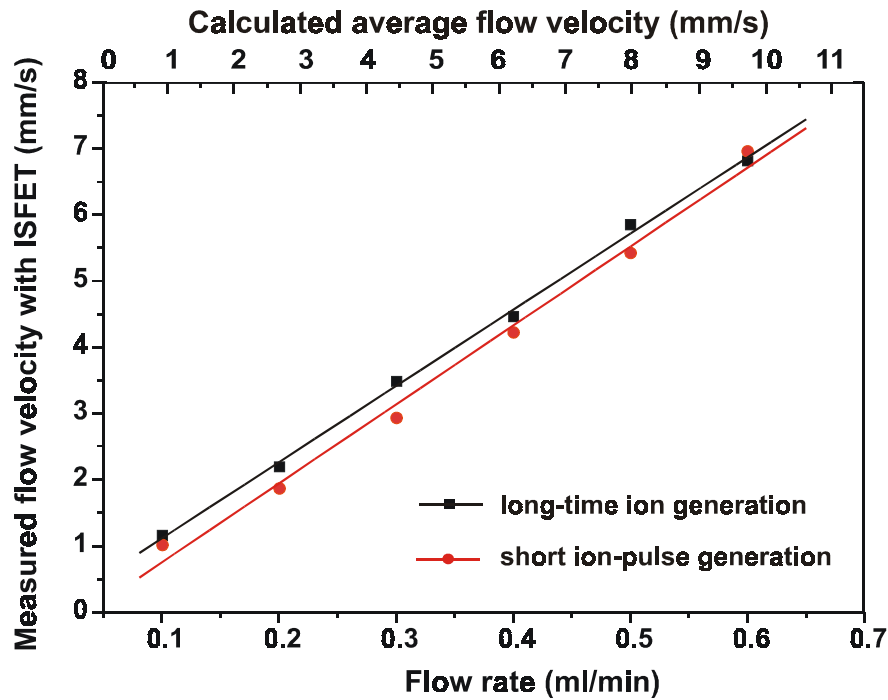
**Figure 4.** Response of the flow-velocity sensor under short ion-pulse generation at different flow rates from 0.1 to 0.5 ml/min (a) and determination of the time of flight (b). In this experiment,  $H^+$  ions were generated at a constant current of  $30 \mu A$  for about 15 s. The arrows mark the time of beginning of ion generation. The time of flight has been evaluated as a time difference  $\Delta t_m$  between the signal maxima of the two ISFETs.

evaluated as the time difference between the signal maxima of the two ISFETs. The corresponding calibration curve of the sensor (Fig. 5) has been obtained using the  $\Delta t_m$  values for different flow rates of the pump.

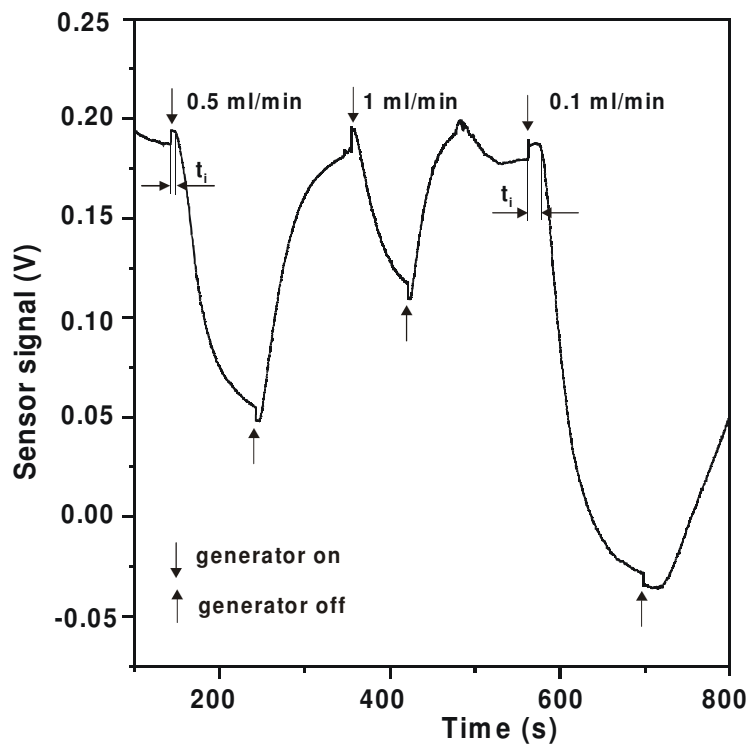
### Calibration curves

Fig. 5 compares the calibration curves of the ISFET-array-based flow-velocity sensor for the two modes of ion generation.

Both curves are nearly identical and demonstrate a good linearity (linear regression coefficients were  $R=0.9991$  and  $R=0.9961$  for the case of long-time and short ion-pulse generation, respectively) between the measured flow velocity with the ISFET array and the delivered flow rate of the pump.



**Figure 5.** Calibration curves of the ISFET-array-based flow-velocity sensor for the two modes of ion generation.



**Figure 6.** Constant-photocurrent-mode response of the LAPS at different flow rates.



However, a procedure of evaluation of the time of flight in the case of the long-time ion generation seems to be relatively complicated. One needs an adequate signal processing electronics and/or software “protocol” that might limit the possible fields of application of the developed flow-velocity sensor. At the same time, for the case of the short ion-pulse generation, the time of flight can be easily evaluated with sufficient accuracy only using the positions of the response curve maxima of the two ISFETs. The measured values of the flow velocity were slightly lower than the calculated (using well-known continuity equation) average velocity values. This can be explained by the flow-velocity profile and the bottom position of the ISFETs in the flow channel.

### **Possibility of flow-velocity measurements with EIS sensor or LAPS**

It is obvious that the proposed concept of an ISFET-based flow-velocity sensor might be also extended to further semiconductor field-effect devices, like capacitive EIS (electrolyte-insulator-semiconductor) sensor or a LAPS (light-addressable potentiometric sensor). Since these three sensor types are based on a common detection principle (semiconductor field effect) and use the same transducer material (usually,  $\text{Ta}_2\text{O}_5$ ,  $\text{Si}_3\text{N}_4$  or  $\text{Al}_2\text{O}_3$  films for pH detection), it can be expected that flow sensors based on an EIS structure or a LAPS should have comparable response characteristics as the ISFET-based flow-velocity sensors. Nevertheless, the sensor fabrication technology and measuring set-up are specific for each type of them. The main advantages of LAPS and EIS sensor over ISFET are the simplicity in the layout, the absence of an encapsulation procedure and thus, the easy and low cost fabrication. On the other hand, the sensitive area of an EIS sensor and a LAPS, in general, is larger than the gate region of an ISFET, which could limit the measuring range of flow velocity. In the case of the LAPS, this drawback can be overcome by using a multi-LAPS or by scanning of the light source. In addition, the flow distribution could also be determined with high resolution.

In this work, the LAPS has been proven for flow-velocity measurements for the first time. A  $\text{Ta}_2\text{O}_5/\text{SiO}_2/\text{p-Si}$  system was used as a pH-sensitive transducer. The chip size of the LAPS was 10 mm x 10 mm and the contact area with the solution was about 5 mm<sup>2</sup>. An LED illuminates the rear side of the sensor at a modulation frequency of 5 kHz. The measurements were carried out by means of constant photocurrent mode [16,17]. Using this mode, the voltage shift, which results from the pH change at the transducer surface during the transportation of the produced  $\text{H}^+$ - and  $\text{OH}^-$ -ions, can be directly recorded.

Fig. 6 demonstrates preliminary results of the response of the LAPS at different flow rates. A long ion-generation mode was applied. Although the response curve is deformed (broadened) due to the large sensitive area of the LAPS, a clear dependence of the delay time  $t_i$  on the flow rate is observed. Thus, these basic experiments could demonstrate also the feasibility of LAPS for flow-velocity measurements.

### **Acknowledgements**

The authors gratefully thank L. Berndsen and J.W. Schultze for valuable discussions and the

Ministerium für Schule, Weiterbildung, Wissenschaft und Forschung des Landes Nordrhein-Westfalen for financial support.

## References

1. Gravesen P.; Branebjerg J.; Jensen O.S. Microfluidics – a review. *J. Micromech. Microeng.* **1993**, *3*, 168-182.
2. Nguyen N.T. Micromachined flow sensors – a review. *Flow Meas. Instrum.* **1997**, *8*, 7-16.
3. Oosterbroek R.E.; Lammerink T.S.J.; Berenschot J.W.; Krijnen G.J.M.; Elwenspoek M.C.; van den Berg A. A micromachined pressure/flow-sensor. *Sens. Actuators A* **1999**, *77*, 167-177.
4. Bergerig O.; Nottmeyer K.; Mizuno J.; Kanai Y.; Kobayashi T. The prandtl micro flow sensor (PMFS): a novel silicon diaphragm capacitive sensor for flow-velocity measurement. *Sens. Actuators A* **1998**, *66*, 93-98.
5. Ashauer M.; Glosch H.; Hedrich F.; Hey N.; Sandmaier H.; Lang W. Thermal flow sensor for liquids and gases based on combinations of two principles. *Sens. Actuators A* **1999**, *73*, 7-13.
6. Wu S.; Lin Q.; Yuen Y.; Tai Y. MEMS flow sensors for nano-fluidic applications. *Sens. Actuators A* **2001**, *89*, 152-158.
7. Glaninger A.; Jachimowicz A.; Kohl F.; Chabicovsky R.; Urban G. Wide range semiconductor flow sensors. *Sens. Actuators A* **2000**, *85*, 139-146.
8. Van Kuijk J.; Lammerink T.S.J.; De Bree H.-E.; Elwenspoek M.; Fluitman J.H.J. Multi-parameter detection in fluid flows. *Sens. Actuators A* **1995**, *46-47*, 369-372.
9. Kruusing A.; Leppävuori S.; Uusimäki A. An ionic liquid flow sensor. *Proceedings of Eurosensors-12*, Southampton, UK, **1998**, pp. 783-786.
10. Khalifa A.J.N.; Mehdi M.M. On the verification of a hydrogen bubble flow meter used for monitoring flow rates in thermosyphon solar water heaters. *Energy Convers. Mgmt.* **1998**, *39*, 1295-1302.
11. Wu J.; Sansen W. Electrochemical time of flight flow sensor. *Sens. Actuators A* **2002**, *97-98*, 68-74.
12. Poghossian A.; Berndsen L.; Lüth H.; Schöning M.J. Novel concept for flow-rate and flow-direction determination by means of pH-sensitive ISFETs. *Proc. SPIE* **2001**, Vol. 4560, 19-27.
13. Poghossian A.; Berndsen L.; Schultze J.W.; Lüth H.; Schöning M.J. "High order" sensor module based on an identical transducer principle and structures. In: M. Butler, P. Vanysek, N. Yamazoe (Eds), *Chemical and Biological Sensors and Analytical Methods*, The Electrochemical Society Inc., Pennington, USA, **2001**, pp. 143-152.
14. Poghossian A.; Berndsen L.; Schöning M.J. Chemical sensor as physical sensor: ISFET-based flow-velocity, flow-direction and diffusion coefficient sensor. *Sens. Actuators B* **2003**, in press.
15. Poghossian A.; Schultze J.W.; Schöning M.J. multi-parameter detection of (bio-)chemical and physical quantities using an identical transducer principle. *Sens. Actuators B* **2003**, *91*, 83-91.
16. Poghossian A.; Yoshinobu T.; Simonis A.; Ecken H.; Lüth H.; Schöning M.J. penicillin detection by means of field effect based sensors: ENFET, capacitive EIS sensor or LAPS? *Sens. Actuators B* **2001**, *237-242*.

17. Yoshinobu, T.; Ecken H.; Poghossian A.; Simonis A.; Iwasaki H., Lüth H., Schöning M.J. Constant-current mode LAPS (CLAPS) for the detection of penicillin. *Electroanalysis* **13**, **2001**, 733-736.

*Sample Availability:* Available from the authors.

© 2003 by MDPI (<http://www.mdpi.net>). Reproduction is permitted for noncommercial purposes.